Correlation of gravestone decay and air quality 1960-2010

Mooers HD[1], Carlson, MJ[1], Harrison, RM[2], Inkpen, RJ[3], and Loeffler, S[4]

1. Department of Earth and Environmental Sciences, University of Minnesota Duluth, 203 Heller Hall, 1114 Kirby Dr., Duluth, MN 55812, USA, email: hmooers@d.umn.edu
2. School of Geography, Earth and Environmental Sciences, University of Birmingham, Birmingham, B15 2TT, United Kingdom; Also at: Department of Environmental Sciences / Center of Excellence in Environmental Studies, King Abdulaziz University, Jeddah, 21589, Saudi Arabia
3. Department of Geography, University of Portsmouth, Buckingham Building, Lion Terrace, Portsmouth, PO1 3HE, United Kingdom
4. Department of Earth Sciences, University of Minnesota Twin Cities, 108 Pillsbury Hall, 310 Pillsbury Dr. SE, Minneapolis, MN, 55455, USA

Highlights

- Gravestone decay provides a quantitative measure of acid flux
- Land use strongly correlated with spatial variability in gravestone decay
- Pronounced increase in deposition efficiency of sulfur dioxide (SO_2) after about 1980

Abstract

Evaluation of spatial and temporal variability in surface recession of lead-lettered Carrara marble gravestones provides a quantitative measure of acid flux to the stone surfaces and is closely related to local land use and air quality. Correlation of stone decay, land use, and air quality for the period after 1960 when reliable estimates of atmospheric pollution are available is evaluated. Gravestone decay and SO_2 measurements are interpolated spatially using deterministic and geostatistical techniques. A general lack of spatial correlation was identified and therefore a land-use-based technique for correlation of stone decay and air quality is employed. Decadally averaged stone decay is highly correlated with land use averaged spatially over an optimum radius of ≈7 km even though air quality, determined by records from the UK monitoring network, is not highly correlated with gravestone decay. The relationships among stone decay, air-quality, and land use is complicated by the relatively low spatial density of both gravestone decay and air quality data and the fact that air quality data is available only as annual averages and therefore seasonal dependence cannot be evaluated. However, acid deposition calculated from gravestone decay suggests that the deposition efficiency of SO_2 has increased appreciably since 1980 indicating an increase in the SO_2 oxidation process possibly related to reactions with ammonia.

Key Words: Gravestone decay; acid deposition; air quality; land use, West Midlands; United Kingdom, SO_2 deposition velocity.

1. Introduction

From the onset of the Industrial Revolution until the environmental revolution of the 1970s Britain was plagued by air pollution from industrial, urban, and residential sources (Sale and Foner, 1993; McCormick, 2013). The largest contributors to air pollution were particulate matter (smoke) and acid in the form of oxides of nitrogen (NO_x) and sulfur (SO_x) compounds, particularly sulfur dioxide (SO_2). (Marsh, 1978; Bricker and Rice, 1993). As early as the 1840s there were efforts to measure air pollution in British cities (Moseley, 2009) and Smith (1876) determined that the burning of coal was the principle source of "acid rain." It was not until about 1960 that the network was greatly expanded with the establishment of the National Survey, which measured daily smoke and sulfur concentrations at over 500 locations (Moseley, 2009). Prior to 1960, air quality measurements were limited in spatial and temporal coverage and often described anecdotally, particularly during severe air quality events. Proxy records have been used to reconstruct air quality; these records include physical descriptions (Allen 1966; Allen 1994; Auliciems and Burton, 1973; Fenger, 2009), particulates in lung tissue samples (Hunt at al. 2003) and sediment cores (Kelly and Thornton, 1996), and lake acidification studies (Battarbee and Renberg, 1990; Battarbee et al., 1990). Air quality measurements are of great interest in studies of ambient environmental conditions (Urone and Schroeder, 1969; Eggleston et al., 1992; Leck and Rodhe, 1989; Fenger, 2009), efficacy of environmental regulation, and health related studies of mortality and morbidity related to acute and chronic respiratory ailments (Macfarlane, 1977; Spix et al. 1993; Ito et al. 1993; Greenstone, 2004).

A proxy that has been used successfully to evaluate historical trends in acid deposition is surface recession of Carrara marble gravestones (Cooke 1989; Cooke et al., 1995; Dragovich, 1991; Inkpen, 1998, 2013; Inpken and Jackson, 2000; Inkpen et al., 2000, 2001, 2008, in press; Meierding, 1981; Mooers et al., 2016; Mooers and Massman, in press; Thornbush and Thornbush, 2013; Viles, 1996), hereafter referred to as gravestone decay to be consistent with the body of recent literature. Mooers et al. (2016) report on a 120-year record of acid deposition in the West Midlands, UK, reconstructed from lead-lettered marble gravestone decay. Their record is compiled from measurements on nearly 600 lead-lettered marble gravestones and they demonstrate that gravestone decay is a robust measure of acid deposition. However, the correlation between acid deposition and available air quality data is more tenuous (Inkpen, 2013; Inkpen et al., in press) and can be influenced by numerous factors (Wesley and Hicks, 1977; Schaefer et al., 1992). Therefore the goal of this study is to explore the relationship between gravestone decay and air quality. Correlation between air quality (SO_2 and smoke) and gravestone decay would then allow quantitative estimation of air quality for earlier periods of time where lead-lettered marble gravestones are available but atmospheric concentrations of pollutants were not measured.

The correlation between surface recession of lead-lettered, Carrara marble gravestones and annually averaged atmospheric SO_2 and smoke measurements in the West Midlands, UK, for the period 1960-2010 is evaluated. The study area includes West Midlands County and surrounding portions of Staffordshire, Worcestershire, and Warwickshire (Figure 1). The industrial and residential development of the area is well documented, there is a large number of cemeteries (Figure 1A) with lead-lettered marble gravestones, and a network of air quality monitoring stations was in place by 1960 (Figure 1B) (Mosley, 2009, 2011). Decadally averaged rates of gravestone decay and measured SO_2 and smoke are interpolated spatially for the period after 1960 and correlation between them is evaluated. Interpolation techniques include deterministic and geostatistical methods; however, because of a high degree of spatial non-stationarity and anisotropy in gravestone decay and limited spatial and temporal coverage of air quality measurements, there is great uncertainly in the interpolated values and correlation between stone decay and air quality is poor.

Because acid deposition is directly related to proximity of sources of SO_2 and NO_x, a land-use based approach for correlation of gravestone decay rates with air quality is developed. Sensitivity and optimization analysis were used to determine the optimum radius of influence of land use on gravestone decay and weighting factors for interpolating intermediate values of decay. In addition, if stone decay is assumed to result primarily from deposition of sulfuric acid then stone decay rates are functions of the production rate of sulfuric acid from SO_2 oxidation. The relationship between stone decay and atmospheric concentration is nonlinear, suggesting a marked increase in the efficiency of the oxidation process of SO_2 after about 1980. The aim of this investigation is therefore to determine the efficacy of gravestone decay in spatially and temporally integrating and recording air quality and explore the nonlinearity of the SO_2 oxidation process.

2. Methods

Mooers et al. (2016) examined the spatial and temporal pattern of acid deposition over the period 1890-2010 from decay of lead-lettered Carrara marble gravestones. Their dataset includes 1417 individual measurements on 591 tombstones in 33 cemeteries collected between 2005 and 2010. The current investigation assesses the correlation of acid deposition and air quality and is more restricted in both space and time. Therefore only the cemeteries within the vicinity of the air quality monitoring network were chosen for analysis (Figure 1A). 21 of the cemeteries reported by Mooers et al. (2016) are used. Additional measurements were taken in July of 2014 to enhance the spatial resolution of gravestone decay over the past 55 years that coincide with air quality monitoring data. 485 inscriptions were measured from 227 tombstones in 10 additional cemeteries with emphasis on post 1950 inscriptions. In addition, Bilston (BIL) Cemetery was revisited and additional data were acquired to constrain post 1950 decay rates. Cemeteries, their locations, and associated data are listed in Table 1.

26 air quality monitoring stations lie in the study area; their locations are shown in Figure 1B and the annually averaged SO_2 and smoke concentrations for all stations are shown in Figure 2. Despite the expansion of the air-quality monitoring network after 1960, there is still a general lack of temporal and spatial continuity of records. The period of record of each monitoring station is highly variable; many stations were only in operation for short periods of time (Table 2).

2.1 Gravestone decay measurements

Gravestones were selected for measurement following the criteria of Mooers et al. (2016), which closely follow the criteria of Cooke et al. (1995). Measured gravestones were standing vertically, had planar surfaces, used lead lettering, had limited ornamentation, and contained two or more inscriptions per stone. In addition, inscriptions had to be in chronological order and there had to be visible evidence that the stone had been resurfaced at the location of each new inscription.

Surface recession of the marble was measured with the depth probe of a digital caliper (accuracy of 0.01mm and precision of ± 0.02mm (instrument error)) from the surface of the lead letters to the stone surface. Resting the digital caliper on two neighboring lead letters provided stability in measurement while reducing error associated with tilting of the depth probe. Ten measurements were made along the date line of each inscription without regard to letter or numeral. Decay for that measurement was then calculated as the trimmed mean (Tukey, 1962) with the high and low values omitted. The trimmed mean was used to avoid bias from unusually large or small values that might result from a variety of causes such as poorly set lettering, odd shaped letters that may hold moisture, etc.

2.2 Determination of Decay Rates

Post 1940 gravestone decay data were plotted vs. inscription date. In general, gravestone decay as a function of time is nonlinear (Mooers and Massman, in press; Mooers et al., 2016) and follows a trend similar to SO_2 and smoke (Figure 2). Gravestone decay rates were therefore determined by best-fit least squares regression function, which in most cases was a 2nd order polynomial. In the case of Rycroft Cemetery in Dudley (DUD) a 3rd order polynomial provided a higher correlation coefficient and prevented the function from becoming slightly negative in the most recent decade Decay rates were then determined as the derivative of the best-fit polynomial at the midpoint of each respective decade.

2.3 Spatial Interpolation of Gravestone Decay

2.3.1 Variogram analysis and Kriging

Since air quality measurements do not coincide geographically with cemeteries, proper spatial interpolation of gravestone decay is critical for comparison. Variograms of the decadally averaged gravestone decay rates from the 33 measured cemeteries were evaluated for best model fit. Stone decay rate for each decade from 1965-2005 was then gridded in ArcGIS® using

Empirical Bayesian Kriging (EBK) at a grid spacing of 200 m. Whereas classical Kriging assumes the estimated semivariogram is the true semivariogram generated from a Gaussian distribution, EBK generates many semivariogram models and removes local trends (Krivourchko, 2012). EBK is particularly well suited for small, moderately non-stationary datasets (Chiles and Delfiner, 1999; Pilz and Spöck, 2007). Interpolated decay rates were compared with air quality data.

2.3.2 Land-use-based approach

Initial variogram analysis suggested that gravestone decay exhibits poor spatial correlation, which is likely an artifact of significant variation in air quality over short spatial scales (Hoek et al., 2002, 2008). Therefore a land-use-based approach was devised to spatially interpolate gravestone decay. Land use was organized into three categories; 1.) urban areas with high concentrations of factories, large buildings and heavy automobile traffic, 2.) residential areas with dense housing and moderate automobile traffic and 3.) rural/green space with few residences and light traffic. Land use was digitized from recent aerial photography and converted to a 200 m grid for analysis. Evaluation of air photos back to 1960 indicates that there have been few major changes in land-use classification. Grid cells were assigned a land-use indicator as follows: green space generates essentially no pollution and was assigned a land-use indicator of 0.0 and urban/industrial areas were assigned a land-use indicator of 1.0. The relation between urban/industrial and residential is less clear but the land-use indicator will lie somewhere between 0 and 1 and this value must be determined through optimization. Three parameters were then optimized: the indicator value of residential land use, the radius of influence contributing to acid deposition at any location, and a weighting parameter to determine the influence of proximal versus distal locations within the optimum radius.

2.4.1 Optimization of Parameters

The initial optimization of weighting of the residential land-use and radius of influence were done using inverse distance weighting as it provides easy variation of parameters. In its simplest form, the inverse distance weighting parameter (w) is

$$w_i(x) = \frac{1}{d(x,x_i)^p} \qquad [1]$$

where *x* is the point where the interpolation is being made, *d* is the distance between known point x_i and the interpolated point, and p is the power parameter. Typical default value for the power parameter for many applications is 2 (inverse distance squared). Reducing the exponent weighs distant points more heavily. For $p=0$ (zero) there is no decrease in weight with distance and the prediction will be simply an average of the values within the search radius. To conduct the initial sensitivity analysis, values of residential land use were varied from 1.0 to 0.0 in steps of 0.2, radius varied from 1 to 10 km, and the inverse distance weighting parameter was varied from 2 to 0. Land use, integrated for each combination of parameters, was calculated for each cell in the 200 m grid. Integrated land use was then correlated with gravestone decay at each cemetery and correlation coefficients (R^2) determined.

Since deterministic methods such as IDW differ in their application from geostatistical and interpolation methods (Zimmerman et al., 1999), several additional techniques of land-use interpolation were employed. These included: ordinary kriging, kernel density, and point density calculations all done within ArcGIS® Geostatistical Analyst® and Spatial Analyst®. For each land-use interpolation method the resulting land-use values at cemeteries were correlated with gravestone decay rate for each decade.

2.4.2 Directional dependence of land-use and gravestone decay rate

The directional dependence of land use on stone decay rate was evaluated by integrating land use within search windows of 90°, 120°, and 180° rotated in 45°, 60°, and 60° degree increments, respectively. For each search window, land-use indicators were calculated at 200 m grid cells using the point density function in ArcGIS® Spatial Analyst®. Calculations were made using optimized parameters for radius and residential land use for each search window. The interpolated land use at each measured cemetery was again correlated with gravestone decay at that point. To evaluate directional trends, rose diagrams were constructed using the mean azimuth of each search window and the correlation coefficient between measured gravestone decay rate and the calculated land-use indicator for each directional search.

2.5 Correlation of gravestone decay rates and measured atmospheric SO_2 and smoke

Two separate sets of interpolated grids of gravestone decay rates were generated. First, decadally averaged decay rates for each cemetery were interpolated spatially using Empirical Bayesian Kriging. Second, the linear least-squares regression equation describing the relation between land use and gravestone decay rate was used to assign decay rates spatially. The interpolated and assigned gravestone decay rates at the location of air quality monitoring stations were then plotted against measured SO_2 and smoke and correlation coefficients (R^2) determined to evaluate the relationship between gravestone decay rates (either spatially interpolated or assigned based on land use) and air quality.

2.6 Evaluation of SO_2 deposition efficiency

Marble gravestone decay is a direct measure of flux density of acid (*F*) (Mooers and Massman, in press), which, in turn, is determined by the atmospheric concentration of pollutants (*C*) at height *z*, and the deposition velocity (v_d) given as

$$v_d = \frac{-F}{C_z}. \qquad [2]$$

SO_2 measurements give us a quantitative measure of the atmospheric concentration. If the stone decay is assumed to result from deposition of sulfuric acid, stone decay rates are a measure of the flux of acid to the stone surface, which is a function of the production rate of sulfuric acid from SO_2 oxidation. It is therefore instructive to plot v_d as a function of time to evaluate temporal changes in deposition velocity (deposition efficiency) of SO_2, which can be affected by a number of factors that influence the correlation of gravestone decay with air quality.

Deposition velocities were calculated at the 26 air quality monitoring stations using the mean annual SO2 concentration and the interpolated gravestone decay rate determined using the optimized land use correlation with gravestone decay. Decay rates were then converted to flux of acid as equivalent SO_2 as

$$F = \dot{e}\rho w_i \frac{M(CaCO_3)}{M(H_2SO_4)}, \qquad [3]$$

where ($\dot{e}$) is decay rate *(l t⁻¹)*, ρ is the density of marble *(M l⁻³)* (we used 2600 kg m^{-3}, Malaga-Starzec et al., (2006)), w_i is the mass fraction of SO_2 in sulfuric acid (0.65), and M($CaCO_3$) and M(H_2SO_4) are the mole weight of calcite (100) and sulfuric acid (98), respectively.

3. Results

3.1 Decay rates

Gravestone decay for the 33 cemeteries included in this study is shown in Figure 3 for the period 1950 to 2010. There is a great deal of variability in decay among stones within any single cemetery. Mooers et al. (2016) conducted an investigation of the sources of variability of stone decay and concluded that by far the largest variability is inherent to the stone. Differences in the physical setting and local effects influence decay by at most a few percent, therefore the data plotted are uncorrected for environmental variables. Time-dependent decay rates were determined by least squares regression (Figure 3, Table 1) for each location.

3.2 Spatial Interpolation of Gravestone Decay

3.2.1 Variogram analysis

Variograms of the decadally averaged gravestone decay rates from the 33 cemeteries for each decade are shown in Figure 4A-E. In all cases the nugget is large compared with the sill, particularly for the 1960s – 1980s, which leads to relative equality in kriging weights and interpolated values are simply averages of known points (Webster and Oliver 1992; University of Salzburg 2014). The ranges in all cases are between 5 and 10 km; this distance is similar to the average distance between measured cemeteries, again suggesting a lack of spatial correlation resulting in simply averaging of known points by kriging. Figure 4F shows the spatially interpolated gravestone decay rates for the 1960s using Empirical Bayesian Kriging gridded at 200 m. The interpolated decay rates were then compared with air quality data from the 11 air quality monitoring stations available in the 1960s; the correlation between interpolated gravestone decay (and therefore acid flux) is poor (Figure 4G) and results for other decades are similar.

3.2.2 Land Use and Optimization of Parameters

Digitized land use is shown in Figure 5 and the results of the optimization of parameters for the land-use analysis using IDW are shown in Figure 6 and Table 3. The correlation between land use and gravestone decay was maximized for an effective radius of approximately 7000m (Figure 6A), a residential land-use indicator of 0.0 (Figure 6B), and an IDW power of < 0.25 with the best correlation at a value of 0.0 (Figure 6C). Therefore the best correlation between land use and gravestone decay is achieved using the same indicator for residential area and green space. Within the study area there are essentially no green spaces larger than 2-3 km in diameter (Figure 5), which is less than half of the calculated effective radius of influence (7000 m) suggesting that air quality in green spaces is likely no different from, and is controlled by, surrounding urban/industrial or residential areas. An optimum inverse distance weighting power of 0.0 indicates that gravestone decay depends basically on an ***average*** of the air quality over a 7000 m radius of the surrounding area. This averaging is consistent with the variogram analysis, which suggested little spatial correlation in the gravestone decay measurements among cemeteries.

Land use was then interpolated to a 200 m grid using ordinary Kriging, kernel density, point density and inverse distance weighting. Figure 7 shows the correlation between the calculated land-use indicator and gravestone decay rate for the various interpolation techniques for a radius of 7000m and a residential land-use indicator of 0.0. Although there is reasonable correlation between land use and stone decay, 4 cemeteries are considered outliers (BEN, COD, JQK, and WAL). Bentley Cemetery (BEN) has an anonymously low decay rate; it is surrounded by four other cemeteries (WIL, WAL, DAR, and BIL) all of which have significantly higher decay rates and far larger number of measurements (Figure 3). Codsall (COD) is anomalously high for the calculated land use, which is mostly rural farmland. Only the relatively small village of Codsall has significant residential neighborhoods. The reason for the anomalously high calculated decay rate is unclear. Key Hill Cemetery (JQK), located in the Birmingham Jewellery Quarter, has anomalously low stone decay compared to Warstone Lane Cemetery, which is located only 100 m away. The dramatic difference in decay rate is attributed to the continuous tree canopy of 100 to150-year-old London plane at Key Hill Cemetery, whereas Warstone Lane Cemetery is largely open (Mooers and Massman, in press; Mooers et al. 2016).

Rrycroft Cemetery (WAL) in Walsall has a relatively high decay rate relative to the calculated land use. Therefore to evaluate the overall effect of these anomalous decay values on the correlation between land use and gravestone decay, BEN, COD, JQK, and WAL were removed from the analysis and the results are shown in Figures 7B, D, F, and H. Note that correlation coefficients are significantly higher with these four outliers omitted.

The highest correlation between the spatially averaged land-use parameter and gravestone decay at measured cemeteries was achieved using point-density analysis and kriging with the omission of the aforementioned four anomalous cemeteries. The point density function simply averages the values within a given radius and kriging, given the poor spatial correlation suggested by variogram analysis, does little more than average the land use over the same radius.

Table 4 shows the correlation coefficients of land-use vs. stone decay rates using the point-density calculation for each decade and for radii of 4000 – 12,000 m. Correlation coefficients are high for 1960s – 1980s at a radius of approximately 6-7 km. The correlation between land use and stone decay drops off after 1990 and the radius of highest correlation increases.

3.2.3 Directional dependence of land use on gravestone decay

The correlation between interpolated land use and gravestone decay rate for the directionally dependent search patterns are shown in Table 5 and Figure 8. Once again omitting BEN, COD, WAL, and JQK from the analysis improves the correlation for the reason stated above. Note that the wider the search pattern the better the correlation between land use and stone decay (Table 5). The correlation coefficients for gravestone decay and land use for each of directional searches are shown in Table 5. Although the correlation coefficients are not as high as the omnidirectional calculation there is a clear directional trend. The highest correlation of land use and gravestone decay for the 1960s and 1970s is south and southwest. From the 1980s to the 2000s the correlation coefficients decrease as the directional dependence of stone decay rate shifts to westerly and then nearly to the north. This change in directional trend coincides with improving air quality and the increase in effective radius of influence contributing acid and changing deposition efficiency of SO_2.

3. 3 Correlation of land use and air quality

The correlation of gravestone decay rate and optimized land use suggests that interpolated land use may be used as a proxy for acid deposition and the relationship between land use and air quality can be evaluated. The decadally averaged SO_2 and smoke concentrations for 23 monitoring stations are shown in Table 6. The correlation of land use (calculated using the point density function, a radius of 7 km, a residential land-use indicator of 0.0) and SO_2 and smoke for the 1960s-1980s is shown in Figure 9. Trends are clearly evident for the 1960s and 1970s even though R^2 values are relatively low. By the 1980s, there is little correlation between land use and SO_2 and smoke.

3.4 Evaluation of SO_2 deposition efficiency

Figure 10 shows the calculated deposition velocities for all air quality monitoring locations for all years (Figure 10). Five-year and ten-year moving averages are also plotted to remove high-frequency variation. Note that after about 1980 there is an increasing trend in the deposition velocity indicating an increase in the efficiency of SO_2 oxidation to sulfuric acid. SO_2 emissions in Europe have decreased substantially since 1980, which has been reflected in large reductions in airborne concentrations of SO_2 (Vestreng et al., 2007). Jones and Harrison (2011) used data from the European Monitoring and Evaluation Programme (EMEP) to examine relationships between SO_2 and sulfate in rural air. The data from all countries examined could be fit to a curvilinear relationship:

$$\chi[SO_4^{2-}] = a \cdot \chi[SO_2]b + c \qquad [4]$$

where $\chi[SO_4^{2-}]$ and $[SO_2]$ are airborne concentrations, and a, b and c are constants. As *b* takes values of typically around 0.6, the percentage reduction in SO_4^{2-} is less than proportionate for a given reduction in SO_2. Hidy et al. (2014) examined measured concentrations from sites in the southeastern United States; between 1999 and 2013, average SO_2 concentrations fell by approximately 84%, while SO_4^{2-} over the same period fell by only 60%. The trend seen in Figure 10 of higher sulfuric acid production efficiency at lower concentrations of SO_2 in more recent years is consistent with this pattern.

4.0 Discussion and Conclusions

Gravestone decay has been shown to serve as an excellent proxy for acid deposition (Mooers et al., 2016; Inkpen, 1998, 2013; Cooke, 1989, Cooke et al., 1995). In addition, the results of this investigation suggest that gravestone decay exhibits a high degree of correlation with interpolated land use (Figure 7), which when integrated over some optimal area essentially determines the pollution sources and therefore the acid flux. The correlation between interpolated land use and air quality, however, is rather poor (Figure 9) and the reasons for the poor correlation are difficult to determine. The paucity of measurements of SO_2 and smoke and the lack of spatial and temporal continuity of the records all contribute to poor correlation. In addition, SO_2 data are annual averages and gravestone decay may well be sensitive to seasonal variations or even short-term extreme events that are not represented in the available data. Correlation between gravestone decay and measured SO_2 and smoke concentrations (air quality) is suggested by their similar exponential trends (Figures 2 and 3). Although spatial interpolation procedures can be used to determine intermediate values of gravestone decay, variogram analysis indicates that there is a lack of spatial correlation particularly prior to about 1980. Local factors, likely related to land use (or possibly even microclimatic effects), therefore appear to overwhelm the spatial continuum. The land-use approach of spatial interpolation is therefore at least as good as other methods even though the correlation with annually averaged annual air-quality data is rather poor.

By about 1980 there was a dramatic turnaround in air quality (Mosley, 2009; 2011) that is evident in both the SO_2 and smoke data (Figure 2) and is well documented in decreasing gravestone decay rates (Mooers et al., 2016) and therefore acid flux. At this time there is a change in the directional dependence of gravestone decay on land use (Figure 8) and an increase in the optimum radius of influence of land use on gravestone decay rates (Tables 3 and 4). Also at this time there appears to be a marked increase in the efficiency of the SO_2 oxidation process (Figure 10). The most probable explanation for the increased deposition efficiency is non-linearity in the SO_2 conversion to sulfate, which is seen in both field measurement data (Jones and Harrison, 2011; Hidy et al., 2014) and numerical model results (Harrison et al., 2013).

An alternative explanation of Figure 10, which needs to be considered, is that increased emissions of nitrogen oxides have led to increased concentrations of nitric acid and higher decay rates. However, UK emission statistics for NO_x show a peak in 1990 with continual decrease until 2013 (National Atmospheric Emissions Inventory, 2016), suggesting that decay due to nitric acid cannot explain the observed trends.

As sulfuric acid production falls in response to decreased SO_2 concentrations, so the extent of neutralization by ammonia is likely to increase, hence reducing sulfate acidity and working in the opposite sense to Figure 10. An alternative role for ammonia is in enhancing the deposition efficiency of SO_2 through co-deposition (Erisman and Wyers, 1993). This is expected to enhance SO_2 deposition efficiency at lower concentrations, and if followed by oxidation of the SO_2 leads to enhanced sulfate concentrations, although not necessarily to sulfuric acid.

As overall air quality improves four trends are evident; 1) the correlation between interpolated land use and stone decay becomes less (Table 4), 2) the effective radius of influence of land use on local air quality increases (Table 4), 3) the directional dependence of land use on local air quality changes from southerly to westerly to northerly, and 4) the efficiency of stone decay increases as SO_2 concentrations fall. These trends are consistent with greatly reduced contrast in air quality among different land-use types. The reason for the change in directional trend from south to north over 50 years is unclear, but possibly related to industrial decline in the Midlands over this time (Spencer et al., 1986).

Finally, interpolated land use and the correlation with SO_2 and smoke can be used to estimate average air quality over the study area for each decade (Figure 11). The improvement in air quality is quite dramatic, particularly between the 1960s and the 1980s. After about the mid-1980s air quality is relatively uniform spatially in the West Midlands and the correlation with land use is significantly lower.

Acknowledgements

Several people were instrumental in the process of gathering data for this study over the past ten years. Tony Sames was our guide and natural historian lending his knowledge and expertise. Special thanks to Liz Ross and Chris and Diane Rance for their logistical support and friendship and to Lillian Mooers for keeping the batteries charged in the canal boat.

References

Allen, C. G., 1966. The Industrial Development of Birmingham and the Black Country 1860-1927, Frank Cass and Co. Ltd., p. 1-479.

Allen, R. C. (1994). Agriculture during the industrial revolution. *The economic history of Britain since, 1700(1),* 96-122.

Auliciems, A., & Burton, I. 1973. Trends in smoke concentrations before and after the clean air act of 1956. *Atmospheric Environment*, 7(11), 1063-1070.

Battarbee, R. W. and Renberg, I., 1990. The Surface Water Acidification Project (SWAP) Palaeolimnology Programme, *Philosophical Transactions of the Royal Society of London*, Series B, Biological Sciences, v. 327, p. 227-232.

Battarbee, R. W., Howells, G., Skeffington, R. A., and Bradshaw, A. D. , 1990. The Causes of Lake Acidification, with Special Reference to the Role of Acid Deposition (and discussion), *Philosophical Transactions of the Royal Society of London*, Series B, Biological Sciences, v. 327, no. 1240, p. 339-347.

Bricker, O. P. and Rice, K. C., 1993. Acid Rain, *Annual Review of Earth Planetary Science*, v. 21, p. 151-174.

Chilès, J-P., and P. Delfiner 1999. Chapter 4 of Geostatistics: Modeling Spatial Uncertainty. New York: John Wiley & Sons, Inc.

Cooke, R. U., 1989. II. Geomorphological Contributions to Acid Rain Research: Studies of Stone Weathering, *Geographical Journal*, v. 155, p. 361-366.

Cooke, R. U., Inkpen, R. J., and Wiggs, G. F. S., 1995. Using Gravestones to Assess Changing Rates of weathering in the United Kingdom, *Earth Surface Processes and Landforms*, v. 20, p. 531-546.

Dragovich, D., 1991. Marble Weathering in an Industrial Environment, Eastern Australia,Environmental *Geology Water Science*, v. 17, no.2, p. 127-132.

Eggleston, S., Hackman, M., Heyes, C., Irwin, J., Timmis, R. & Williams, M., 1992. Trends in urban air pollution in the United Kingdom during recent decades. *Atmospheric Environment*, 26B (2), 227-239.

Erisman, J. W. and Wyers, G. P., 1993. Continuous measurements of surface exchange of SO_2, and NH3; implications for their possible interaction in the deposition process. *Atmospheric Environment,* 37A, 1937-1949.

Fenger, J., 2009. Air pollution in the last 50 years – From local to global. *Atmospheric Environment*, 43, 13-22.

Greenstone, M., 2004. Did the Clean Air Act cause the remarkable decline in sulfur dioxide concentrations? *Environmental Economics and Management* 47, 585-611

Harrison, R. M., Jones, A. M., Beddows, D. and Derwent, R. G., 2013. The effect of varying primary emissions on the concentrations of inorganic aerosols predicted by the enhanced UK photochemical trajectory model. *Atmospheric Environment*, 69, 211-218.

Hidy, G. M., Blanchard, C. L., Baumann, K., Edgerton, E., Tanenbaum, S., Shaw, S., Knipping, E., Tombach, I., Jansen, J. and Walters, J., 2014. Chemical climatology of the southeastern United States, 1999-2013. *Atmospheric Chemistry & Physics*, 14, 11893-11914.

Hoek, G., Meliefste, K., Cyrys, J., Lewne, M., Bellander, T., Brauer, M., Fischer, P., Gehring, U., Heinrich, J., van Vliet, P., Brunekreef, B., 2002. Spatial variability of fine particles concentrations in three European areas. *Atmospheric Environment*. 36, 4077–4088.

Hoek, G., Beelen, R., De Hoogh, K., Vienneau, D., Gulliver, J., Fischer, P., & Briggs, D. (2008). A review of land-use regression models to assess spatial variation of outdoor air pollution. *Atmospheric Environment*, 42(33), 7561-7578.

Hunt, A., Abraham, J., Judson, B. and Berry, C., 2003. Toxicologic and Epidemiologic Clues from the Characterization of the 1952 London Smog Fine Particulate Matter in Archival Autopsy Lung Tissues. *Environmental Health Perspectives*, 111(9), 1209-1214

Inkpen, R. J. and Jackson, J., 2000. Contrasting Weathering Rates in Coastal, Urban and Rural Areas in Southern Britain: Preliminary Investigations Using Gravestones. *Earth Surface Processes and Landforms*, v. 25, p. 229-238.

Inkpen, R. J., 1998. Gravestones: Problems and potentials as indicators of recent changes in weathering, in Jones, M. and Wakefield, R. (eds.), Aspects of stone weathering, decay and conservation, Imperial College Press, London, p. 16-27.

Inkpen, R., 2013. Reconstructing past atmospheric pollution levels using gravestone erosion rates. *Area*, 45(3), 321-329.

Inkpen, R. J., & Jackson, J., 2000. Contrasting weathering rates in coastal, urban and rural areas in southern Britain: preliminary investigations using gravestones. *Earth Surface Processes and Landforms*, 25(3), 229-238.

Inkpen, R. J., Collier, P., and Fontana, D., 2000. Close-Range Photogrammetric Analysis of Rock Surfaces. *Zeitschrift fur Geomorphologie Supplementband* (120). pp. 67-81.

Inkpen, R. J., Fontana, D., and Collier, P., 2001. Mapping Decay: Integrating Scales of Weathering within a GIS. *Earth Surface Processes and Landforms*, v. 26, p. 885¬900.

Inkpen, R., Duane, B., Burdett, J., & Yates, T., 2008. Assessing stone degradation using an integrated database and geographical information system (GIS). Environmental geology, 56(3-4), 789-801.

Inkpen, R.J., Mooers, H.D., and Carlson, M.J., in press, Using rates of gravestone decay to reconstruct atmospheric sulphur dioxide levels. *Area*.

Ito, K., Thurston, G., Hayes, C. & Lippmann, M., 1993. Associations of London, England, Daily mortality with particulate matter, sulfur dioxide, and acidic aerosol pollution. *Archives of Environmental Health*, 48(4), 213-220.

Jones, A. M., Harrison and R. M., 2011. Temporal trends in sulphate concentrations at European sites and relationships to sulphur dioxide. *Atmospheric Environment*, 45, 873-882.

Kelly, J. and Thornton, I., 1996. Urban Geochemistry: A study of the influence of anthropogenic activity on the heavy metal content of soils in traditionally industrial and non-industrial areas of Britain. *Applied Geochemistry*, 11, 363-370.

Krivourchko, K., 2012. Empirical Bayesian Kriging. http://www.esri.com/news/arcuser/1012/empirical-byesian-kriging.html.

Leck, C. & Rodhe, H., 1989. On the relation between anthropogenic SO2 emissions and concentration of sulfate in air and precipitation. *Atmospheric Envrionment*, 23 (5), 959-966.

Macfarlane, A., 1977. Daily mortality and environment in English conurbations; 1: Air pollution, low temperature, and influenza in Greater London. *British Journal of Preventative and Social Medicine*, 31, 54-61.

Malaga-Starzec, K., Åkesson, U., Lindqvist, J.E., Schouenborg, B., 2006. Microscopic and macroscopic characterization of the porosity of marble as a function of temperature and impregnation. *Construction and Building Materials*. 20 (10), 939-947.

Marsh, A.R.W., 1978. Sulphur and nitrogen contributions to the acidity of rain. *Atmospheric Environment*, vol. 12, pp 401-406.

McCormick, J., 2013. British Politics and the Environment. Routledge.

Meierding, T. C., 1981. Marble Tombstone Weathering Rates, A Transect of the United States. *Physical Geography*, v. 2, 18 p.

Mooers, H.D. and Massman, W.J., in press, Gravestone decay and the determination of deciduous bulk canopy resistance to acid deposition. *Science of the Total Environment.*

Mooers, H.D., Cota-Guertin, A.R., Regal, R.R., Sames, A.R., Dekan, A.J., and Henlels, L.M., 2016. A 120-year record of the spatial and temporal distribution of gravestone decay and acid deposition, *Atmospheric Environment* 127, 139-154

Mosley, S., 2009. A network of trust: Measuring and monitoring air pollution in British cities, 1912-1960. *Environment and History*, 15, 273-302.

Mosley, S., 2011. Environmental history of air pollution and protection. World Environmental History, Encyclopedia of Life Support Systems.

National Atmospheric Emissions Inventory, 2016. http://naei.defra.gov.uk/.

Pilz, J., and G. Spöck, 2007. Why Do We Need and How Should We Implement Bayesian Kriging Methods. *Stochastic Environmental Research and Risk Assessment* 22 (5): 621–632.

Sale, K., & Foner, E. (1993). *The Green Revolution: The Environmental Movement 1962-1992* (Vol. 1). Macmillan.

Schaefer, D.A., Conklin, P., Knoerr, K., 1992a. Atmospheric deposition of acid. In: Johnson, D.W., Lindberg, S.E. (Eds.), Atmospheric Deposition and Forest Nutrient Cycling. Springer-Verlag, New York, p. 427-444.

Smith, R.A., 1876. What Amendments are Required in the Legislation Necessary to Prevent the Evils Arising from Noxious Vapours and Smoke? *Transactions of the National Association for the Promotion of Social Science*: 495–542.

Spencer, K., 1986. Crisis in the industrial heartland: a study of the West Midlands. Oxford University Press, USA.

Spix, C., Heinrich, J., Dockery, D., Schwartz, J., Volksch, G., Schwinkowski, K., Collen, C., Wichmann, H. E., 1993. Air pollution and daily mortality in Erfurt, East Germany, 1980-1989. *Environmental Health Perspectives*, 101 (6), 518-526.

Thornbush, M.J., Thornbush, S.E., 2013. The application of a limestone weathering index at churchyards in central Oxford, UK. *Applied Geography*. 42, 157e164.

Tukey, J.W., 1962. The future of data analysis. *Ann. Math. Stat*., 1–67.

University of Salzburg, 2014. Interfaculty Department of Geoinformatics - Z_GIS, Austria, http://www.unigis.ac.at/fernstudien/UNIGIS_professional/traun/spatial_interpolation/kriging3.htm.

Vestreng, V., Myhre, G., Fagerli, H., Reis, S. and Tarrason, L., 2007. Twenty-five years of continuous sulphur dioxide emission reduction in Europe. *Atmospheric Chemistry & Physics*, 7, 3663-3681.
Viles, H., 1996. Unswept stone, besmeer'd by sluttish time: air pollution and building stone decay in Oxford, 1790e1960. *Environmental History* 2 (3), 359e372.
Webster, R., & Oliver, M. A., 1992. Sample adequately to estimate variograms of soil properties. *Journal of Soil Science*, 43(1), 177-192.
Wesely, M. L., & Hicks, B. B., 1977. Some factors that affect the deposition rates of sulfur dioxide and similar gases on vegetation. *Journal of the Air Pollution Control Association*, 27(11), 1110-1116.
Zimmerman, D., Pavlik, C., Ruggles, A., and Armstrong, M.P., 1999. An Experimental Comparison of Ordinary and Universal Kriging and Inverse Distance Weighting, *Mathematical Geology*, Vol. 31, No. 4, 1999.

Figure 1. West Midlands County, UK, showing the locations of cemeteries (A) and air-quality monitoring stations (B).

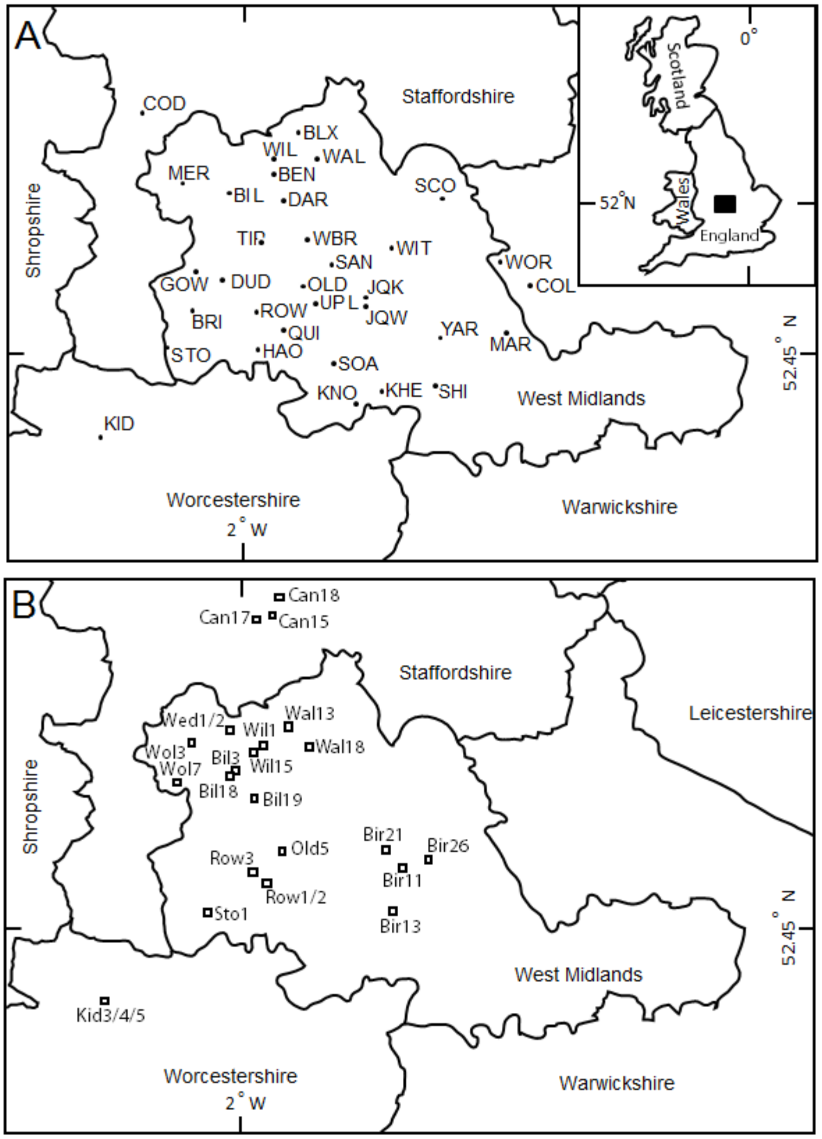

Figure 2. SO_2 and smoke concentrations from all stations for the period 1960 to 2005, the period of available record. Each data point represents a one-year average of SO_2 or smoke for the 23 stations listed in Table 2.

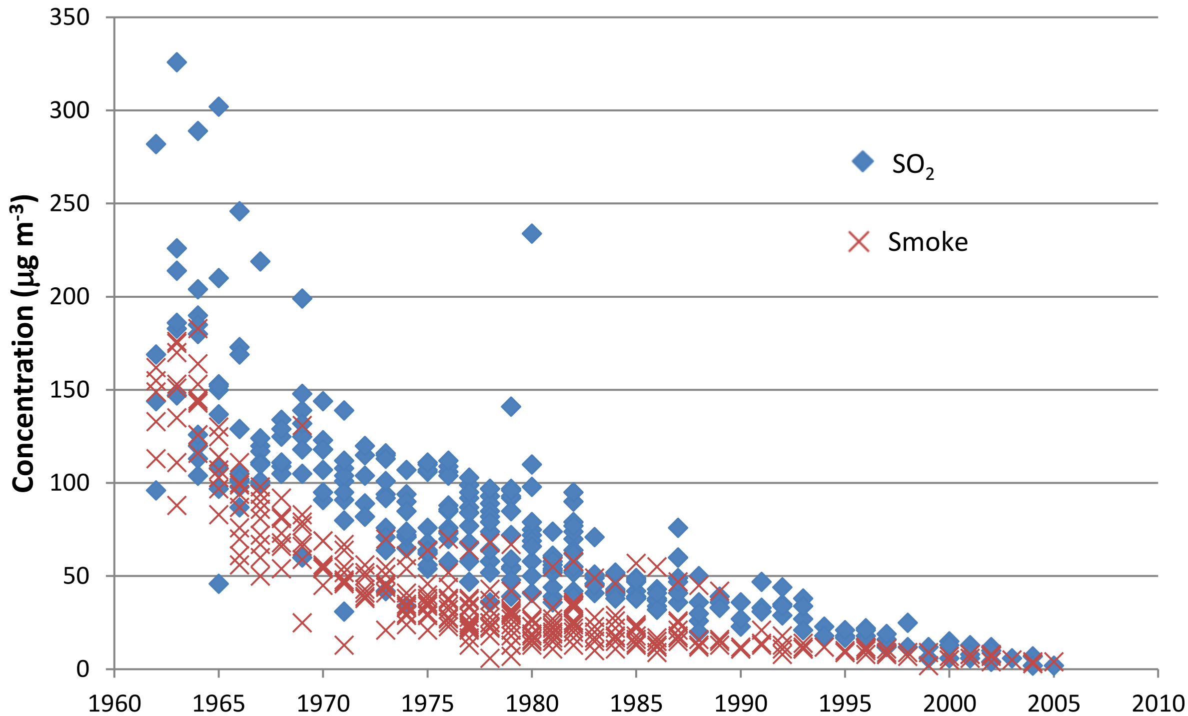

Figure 3. Gravestone decay for 33 cemeteries in the West Midlands and surrounding area. Each point represents stone decay on a single inscription. Values are the average of 10 measurements on the date line of the inscription with the high and low values removed (trimmed mean). Data are plotted as years before 2010 so that regression equations pass through the graph origin.

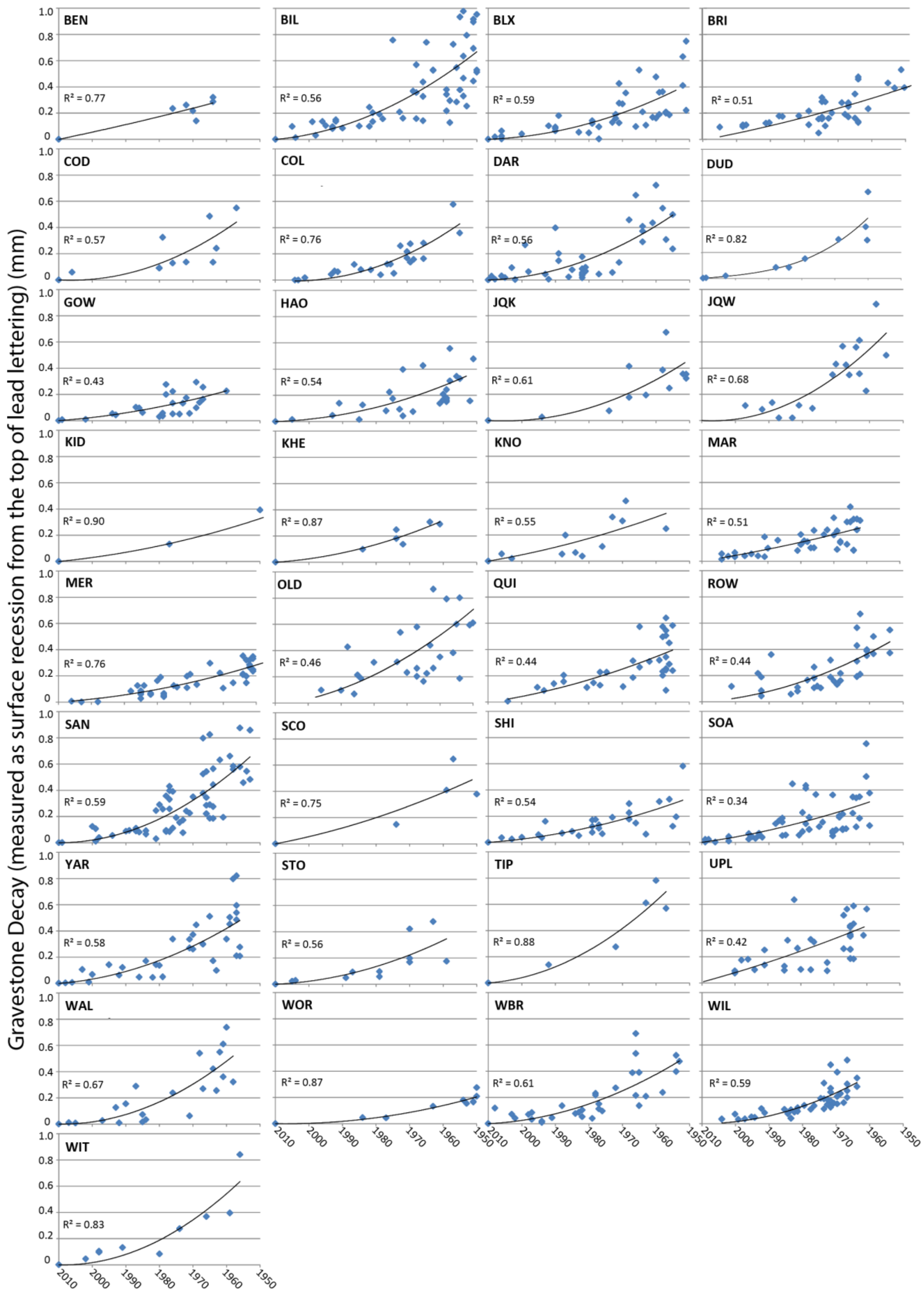

Figure 4. A-E) variograms of the gravestone decay rate for the 1960s – 2000s, respectively; F) results of Empirical Bayesian Kriging of decay rates, and G) correlation of interpolated gravestone decay rate and SO_2 concentrations at air quality monitoring locations.

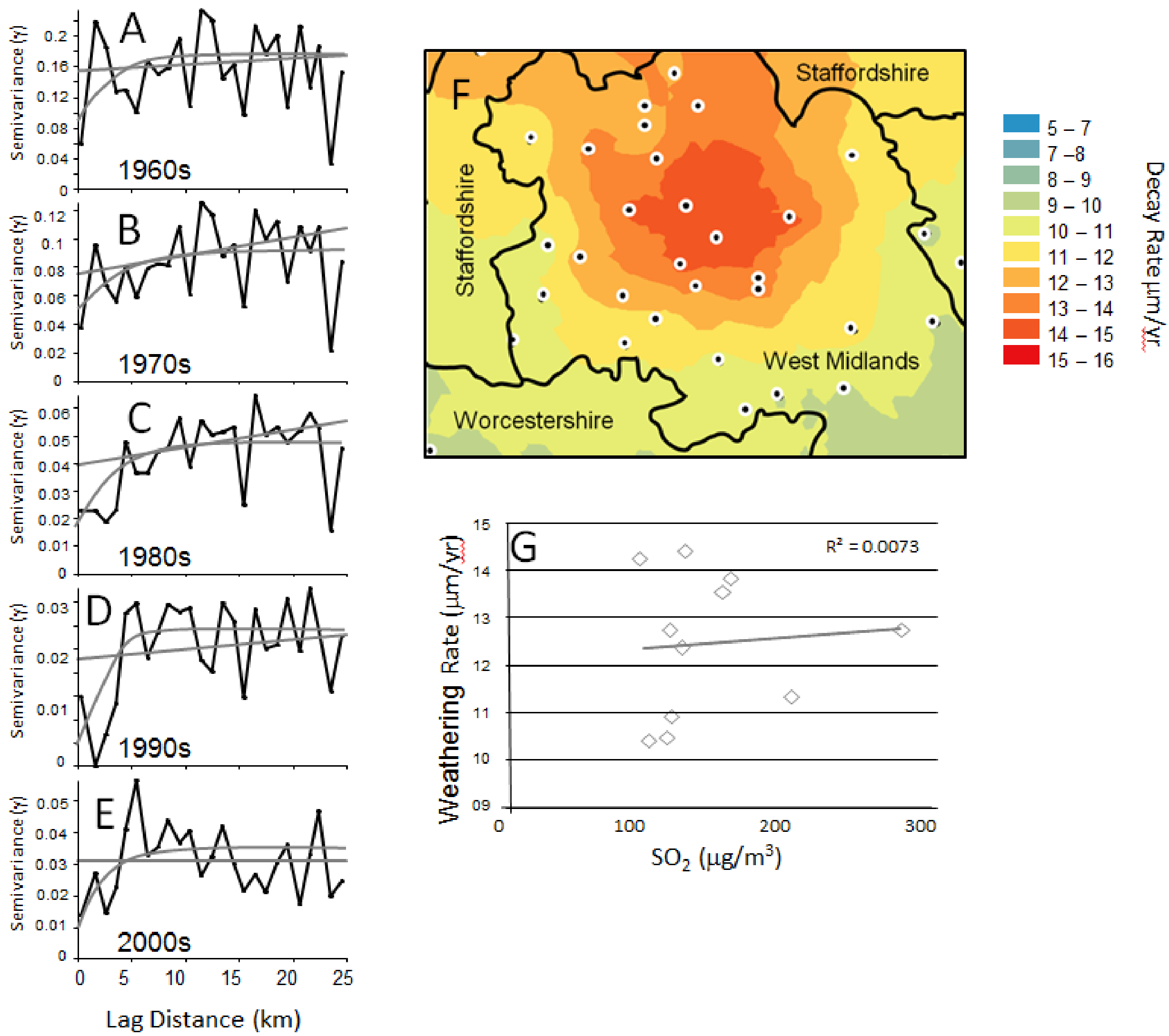

Figure 5. Land use digitized from recent aerial photography.

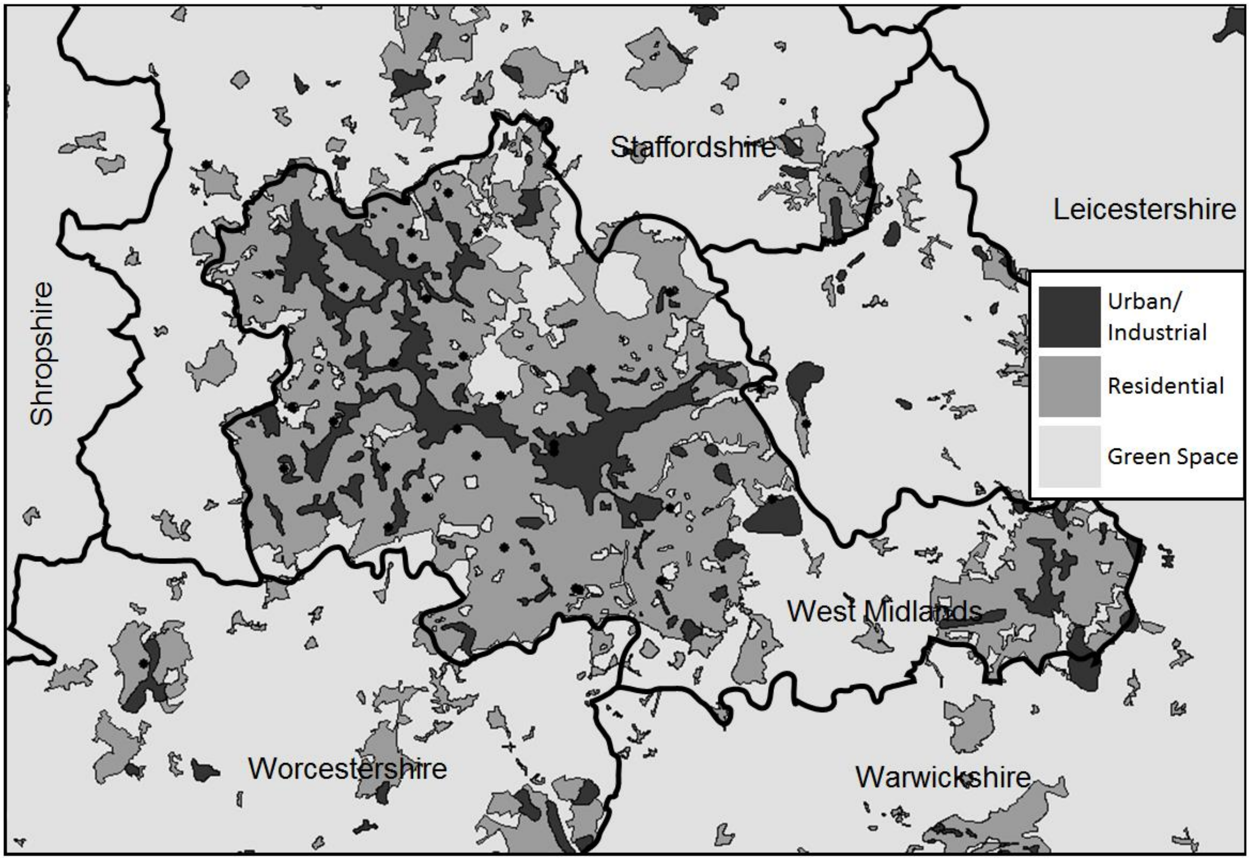

Figure 6. IDW optimization; A) radius, B) residential land-use indicator, and C) inverse-distance weighting factor.

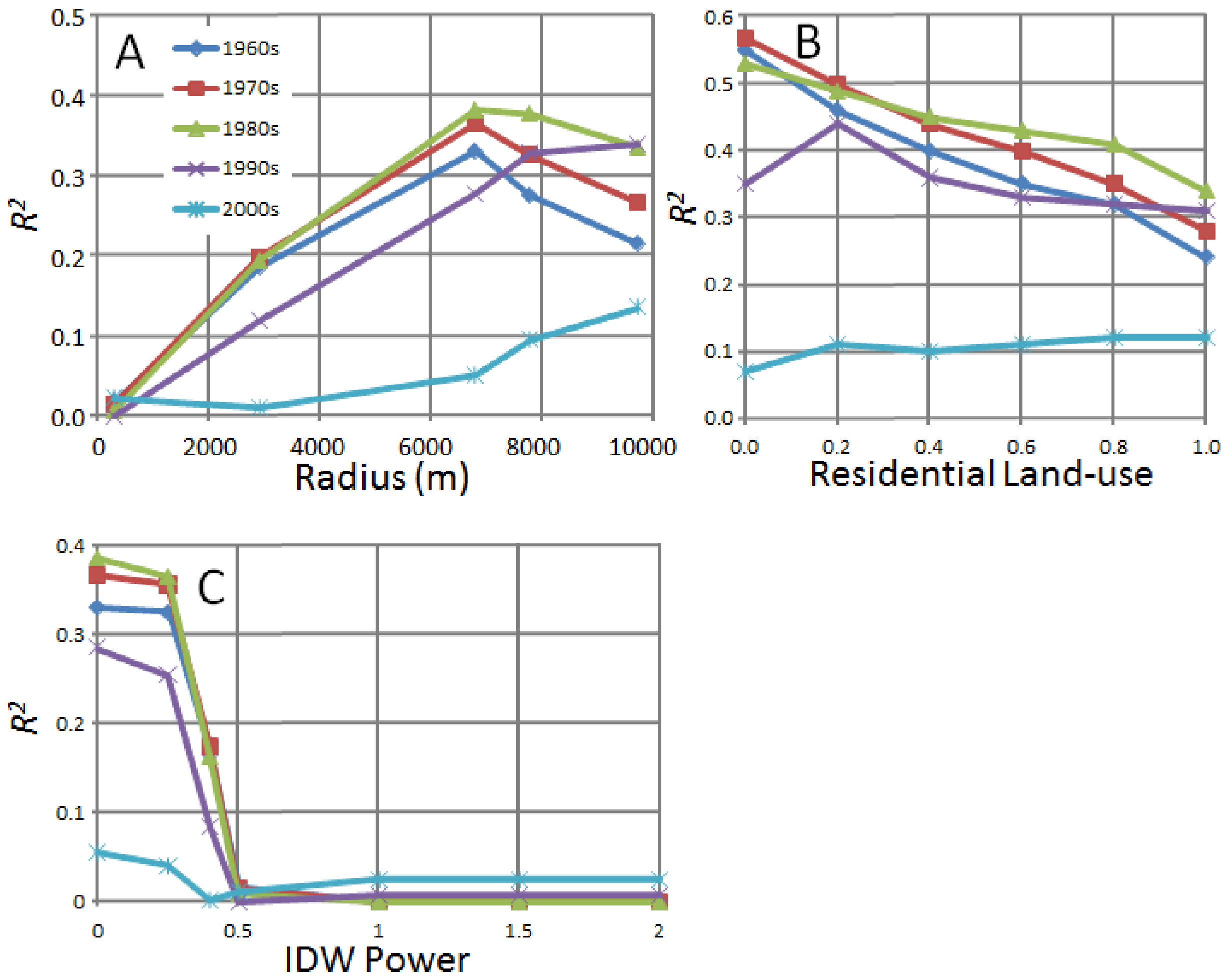

Figure 7. Relationship between Interpolated land use and gravestone decay rate for 33 cemeteries. Land-use interpolation by Kriging (A, B), Kernel Density (C,D), Point Density (E,F), and IDW (G,H). For each method of interpolation the correlation coefficient is greatly improved by omitting the four anomalous cemeteries as described in the text (B, D, F, and H).

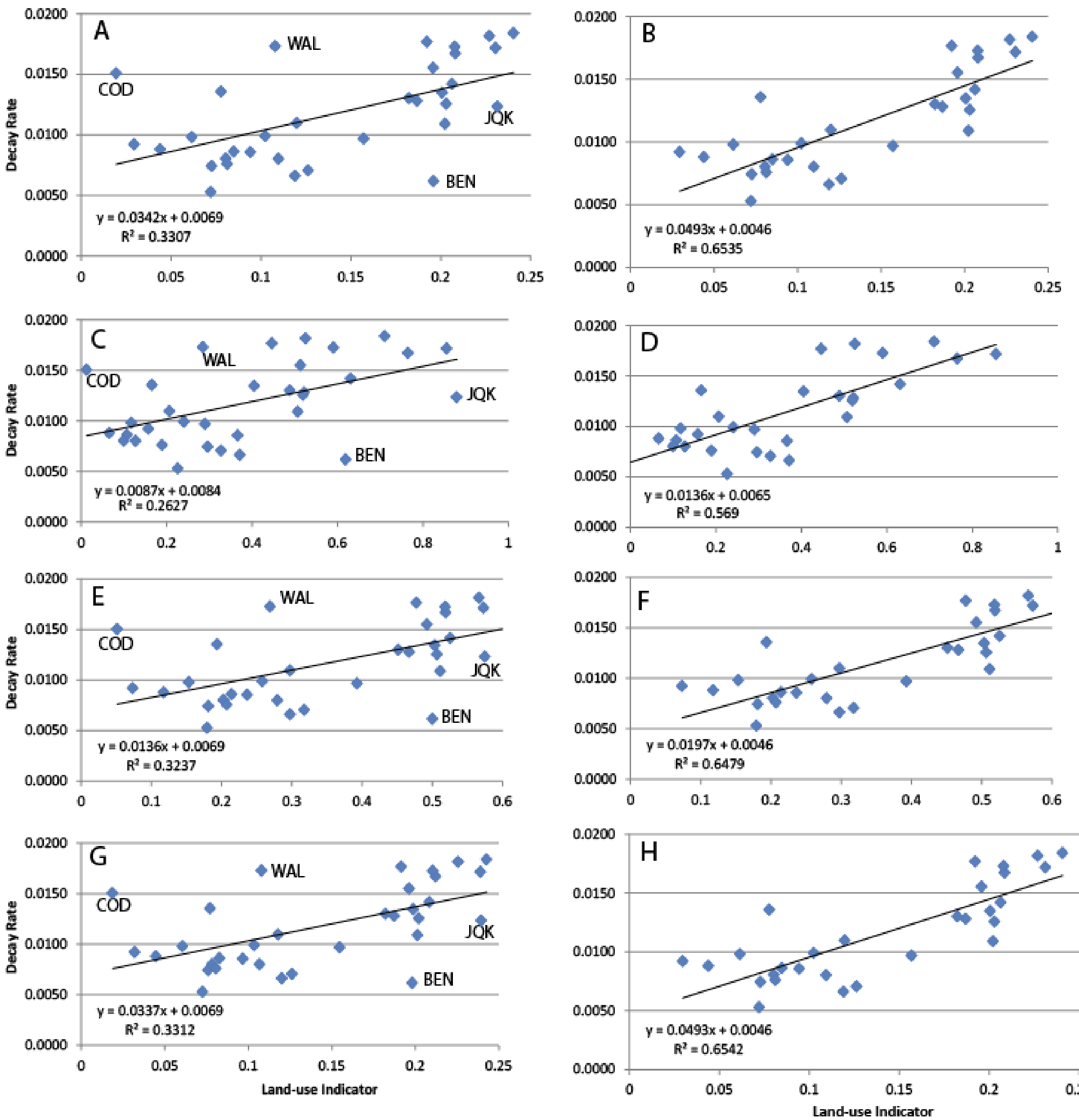

Figure 8. Rose diagrams of directional dependence of land use on gravestone weathering rate. Diagrams were constructed from the directional searches using the mean azimuth of each search and the correlation coefficient for that search window between gravestone weathering and the interpolated land-use indicator.

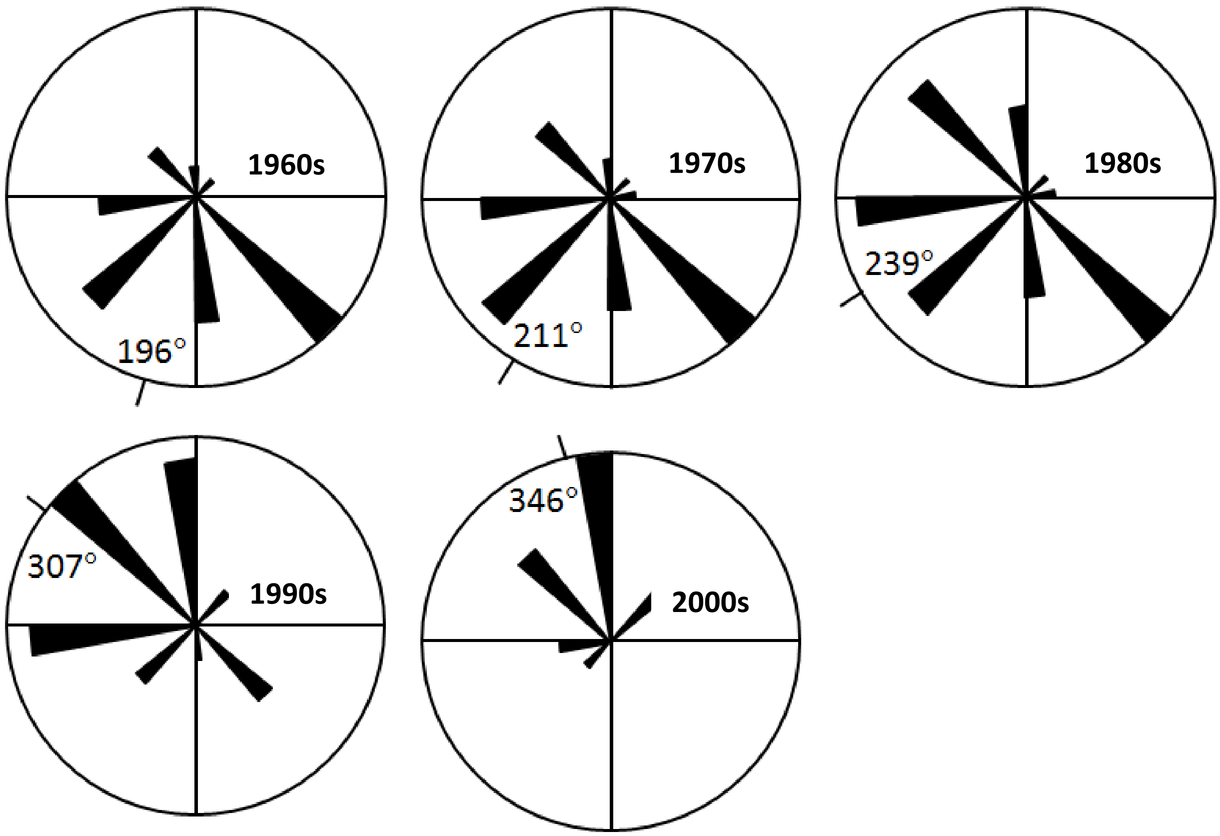

Figure 9. Correlation between land-use indicator and SO_2 and smoke concentrations for the 1960s (A, B), 1970s (C, D), and the 1980s (E, F).

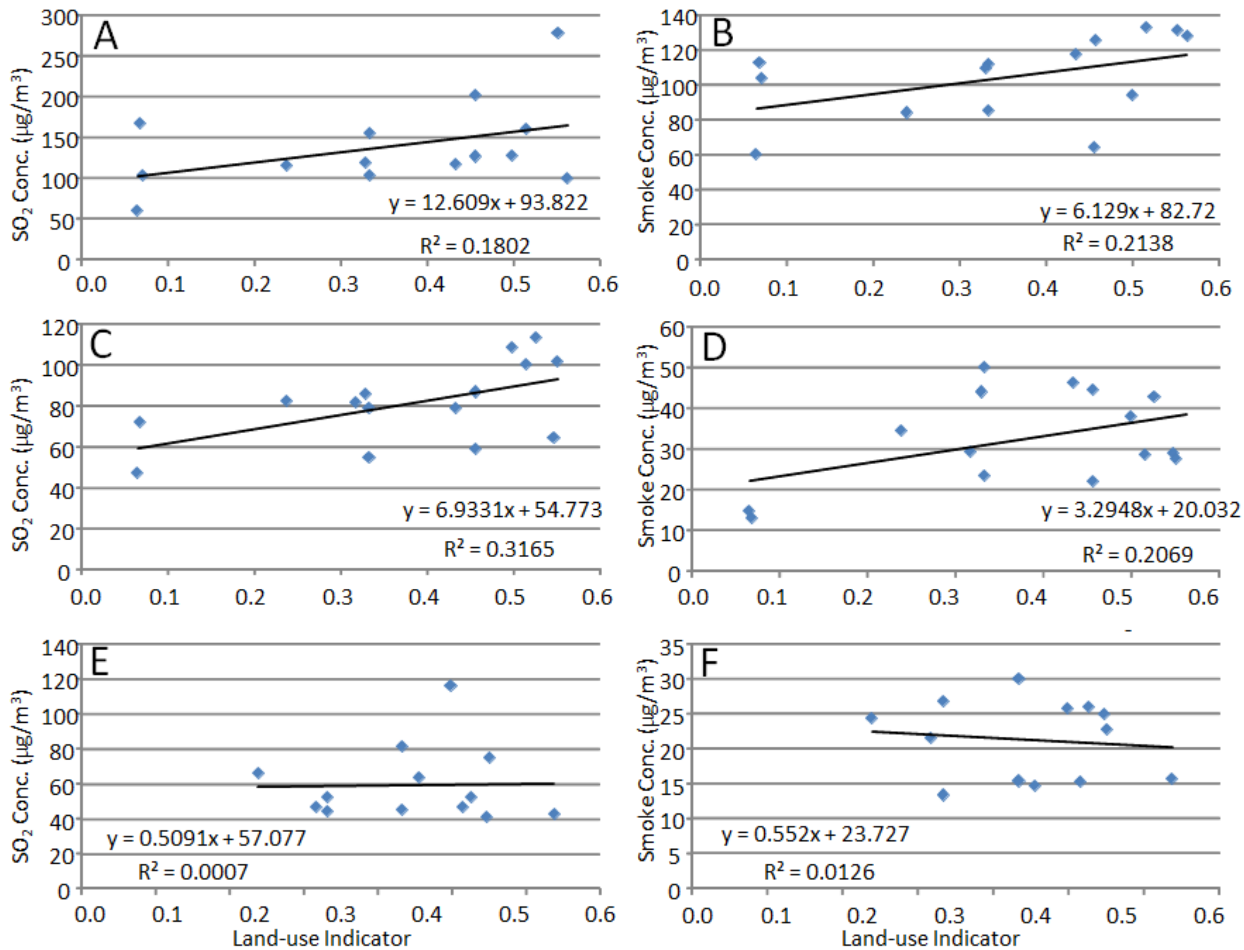

Figure 10. Surrogate deposition velocity (F/C_z) as a function of year of measurement. Blue diamonds are all data, red squares are 5-year and green triangles are 10-year moving averages. Trend line was calculated from all data points using a third-order polynomial least-squares regression.

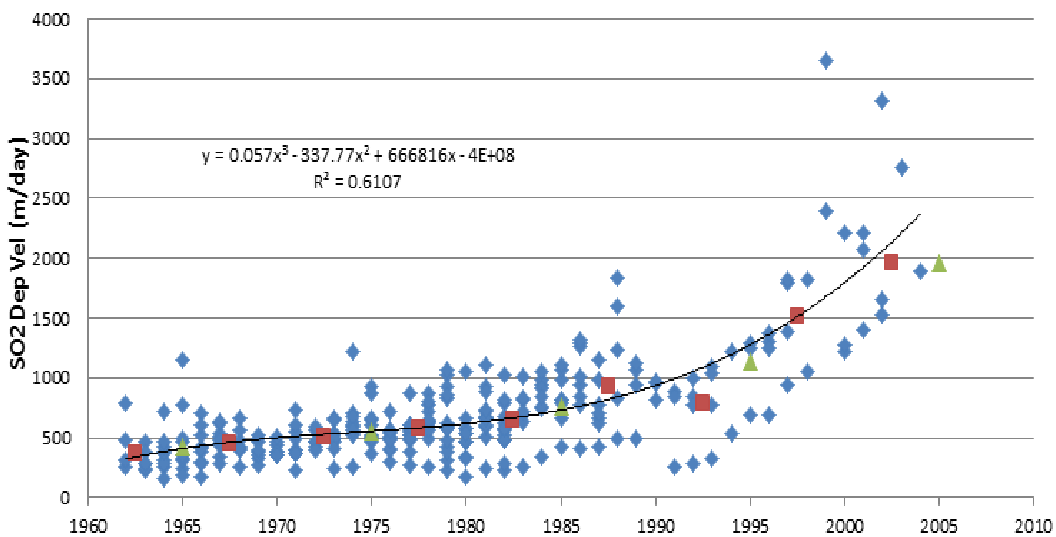

Figure 11. Predicted SO_2 and smoke concentrations based on land-use/air quality correlations in Figure 9 for the 1960s through 1980s.

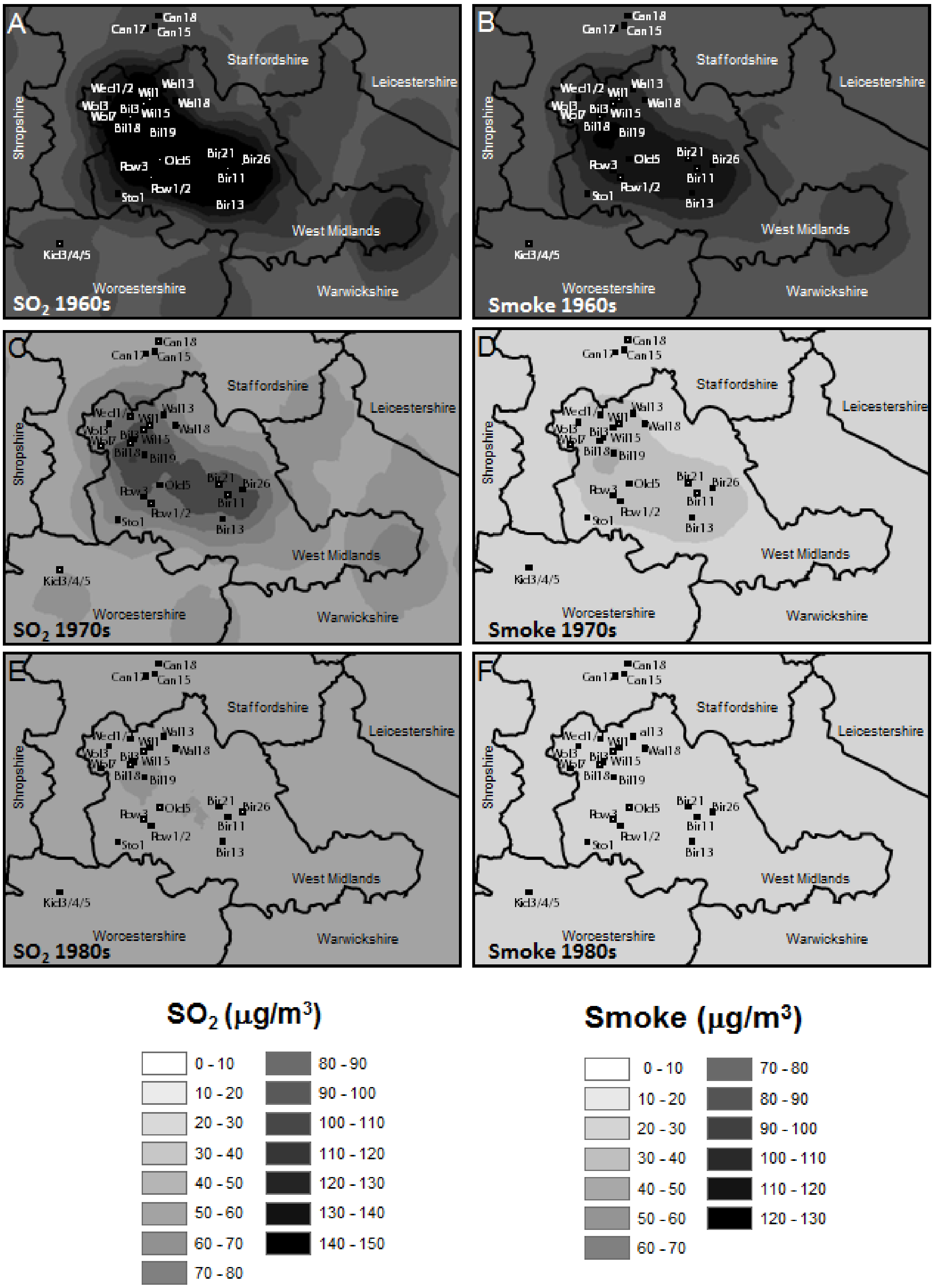

Table 1. List of cemeteries visited during this investigation. Locations are given in UTM Zone 30. Gravestone decay vs. age for each cemetery was fitted with a non-linear polynomial regression and the equation and *R2* value are tabulated. For each decade 1960-2010 mean decay rates were calculated at the derivative of the regression equation for the midpoint year and are given in μm/yr.

Identifier	Cemetery Name	Easting	Northing	Neighborhood	Function	R2	*Y2000s*	*Y1990s*	*Y1980s*	*Y1970s*	*Y1960s*
BEN	Bentley Cemetery	565735	5826699	Bentley	$y = 1.51E-05\ X^2 + 5.32E-03\ X + 0$	$R^2 = 0.77$	0.0041	0.0046	0.0051	0.0057	0.0062
BIL	Bilston Cemetery	561866	5825044	Bilston	y = 1.47E-04 X2 + 2.34E-03 X + 0	$R^2 = 0.55$	0.0050	0.0079	0.0108	0.0138	0.0167
BLX	Bloxwich Cemetery	567804	5830398	Bloxwich	y = 1.02E-04 X2 + 9.82E-04 X + 0	$R^2 = 0.59$	0.0028	0.0049	0.0069	0.0089	0.0110
BRI	Brierly Cemetery	558519	5814794	Brierly	$y = 9.36E-05\ X^2 - 6.09E-04\ X + 0$	$R^2 = 0.53$	0.0011	0.0029	0.0048	0.0067	0.0086
COD	Saint Nicholas Churchyard	554119	5831975	Codsall	y = 1.82E-04 X2 - .28E-03 X + 0	$R^2 = 0.57$	0.0005	0.0042	0.0078	0.0114	0.0151
COL	Coleshill Parish Church/Cemetery	588007	5817313	Coleshill	y = 1.73E-04 X2 - 2.02E-03 X + 0	$R^2 = 0.76$	0.0000	0.0032	0.0066	0.0101	0.0136
DAR	Fallings Heath Cemetery	566570	5824432	Darlston	y = 1.48E-04 X2 + 8.28E-04 X + 0	$R^2 = 0.56$	0.0023	0.0053	0.0082	0.0112	0.0142
DUD	Scot's Green Cemetery	561285	5817504	Dudley	$y = 3.24E-06\ X^3 - 03E-05\ X^2 + 0.002\ X + 0$	$R^2 = 0.82$	0.0014	0.0024	0.0051	0.0094	0.0155
GOW	Gornal Woods Cemetery	558912	5818302	Gornal Woods	$y = 5.22E-05\ X^2 + 1.94E-03\ X + 0$	$R^2 = 0.43$	0.0029	0.0039	0.0050	0.0060	0.0071
HAO	Halesowen Cemetery	564377	5811518	Halesowen	$y = 9.26E-05\ X^2 + 21E-04\ X + 0$	$R^2 = 0.54$	0.0025	0.0043	0.0062	0.0080	0.0099
JQK	Key Hill Cemetery	573743	5816222	Jewellery Quarter	$y = 1.52E-04\ X^2 - 1.40E-03\ X + 0$	$R^2 = 0.61$	0.0001	0.0032	0.0062	0.0093	0.0123
JQW	Warstone Lane Cememtery	573730	5815781	Jewellery Quarter	$y = 2.48E-04\ X^2 - 1.49E-03\ X + 0$	$R^2 = 0.68$	0.0011	0.0051	0.0091	0.0132	0.0172
KID	Kidderminster Cemetery	550592	5803814	Kidderminster	$y = 4.95E-05\ X^2 + 2.47E-03\ X + 0$	$R^2 = 0.90$	0.0015	0.0034	0.0054	0.0073	0.0092
KHE	Brandwood End Cemetery	574978	5808054	Kings Heath	$y = 9.29E-05\ X^2 + 1.74E-03\ X + 0$	$R^2 = 0.87$	0.0009	0.0028	0.0048	0.0067	0.0086
KNO	Saint Nicholas Cemetery	575167	5807964	Kings Norton	$y = 4.72E-05\ X^2 + 4.37E-03\ X + 0$	$R^2 = 0.55$	0.0030	0.0043	0.0055	0.0068	0.0080
MAR	Marston Green Burial Grounds	586086	5813062	Marston Green	$y = 2.54E-05\ X^2 + 4.08E-03\ X + 0$	$R^2 = 0.51$	0.0048	0.0045	0.0049	0.0058	0.0074
MER	Merridale Cemetery	557690	5825788	Merridale	$y = 4.98E-05\ X^2 + 1.73E-03\ X + 0$	$R^2 = 0.76$	0.0026	0.0036	0.0046	0.0056	0.0066
OLD	Olbury Cemetery	568314	5817067	Oldbury	$y = 1.48E-04\ X^2 + 2.74E-03\ X + 0$	$R^2 = 0.46$	0.0054	0.0084	0.0113	0.0143	0.0173
QUI	Quinton Cemetery	566553	5813148	Quinton	$y = 5.76E-05\ X^2 + 4.03E-03\ X + 0$	$R^2 = 0.44$	0.0051	0.0062	0.0074	0.0085	0.0097
ROW	Rowley Regis Cemetery	564247	5814857	Rowley Regis	$y = 1.10E-04\ X^2 + 2.04E-03\ X + 0$	$R^2 = 0.44$	0.0040	0.0062	0.0084	0.0106	0.0128
SAN	Handsworth Cemetery	570750	5818928	Sandwell	$y = 2.02E-04\ X^2 + 1.85E-05\ X + 0$	$R^2 = 0.59$	0.0020	0.0061	0.0101	0.0141	0.0182
SCO	Sutton Coldfield Cemetery	580327	5824737	Sutton Coldfield	$y = 5.85E-05\ X^2 + 4.90E-03\ X + 0$	$R^2 = 0.75$	0.0033	0.0047	0.0061	0.0074	0.0088
SHI	Robin Hood Cemetery and Crematorium	579776	5808467	Shirley	$y = 6.34E-05\ X^2 + 1.88E-03\ X + 0$	$R^2 = 0.54$	0.0025	0.0038	0.0050	0.0063	0.0076
SOA	Lodge Hill Cemetery and Crematorium	570966	5810346	Selly Oak	$y = 5.07E-05\ X^2 + 3.65E-03\ X + 0$	$R^2 = 0.34$	0.0040	0.0050	0.0060	0.0070	0.0080
YAR	South Yardley Cemetery and Crematorium	580324	5812585	South Yardley	$y = 1.27E-04\ X^2 + 2.05E-03\ X + 0$	$R^2 = 0.58$	0.0033	0.0059	0.0084	0.0109	0.0135
STO	Stourbridge Crematorium	556494	5811652	Stourbridge	$y = 1.10E-04\ X^2 + 1.18E-03\ X + 0$	$R^2 = 0.56$	0.0008	0.0031	0.0053	0.0076	0.0098
TIP	Tipton Cemetery	564697	5820810	Tipton	$y = 2.11E-04\ X^2 + 1.97E-03\ X + 0$	$R^2 = 0.88$	0.0014	0.0057	0.0099	0.0141	0.0184
UPL	Uplands Cemetery	569384	5815531	Uplands	$y = 3.94E-05\ X^2 + 7.03E-03\ X + 0$	$R^2 = 0.42$	0.0077	0.0085	0.0093	0.0101	0.0109
WAL	Ryecroft Cemetery	569438	5828132	Walsall	$y = 1.96E-04\ X^2 - 3.38E-04\ X + 0$	$R^2 = 0.69$	0.0016	0.0055	0.0095	0.0134	0.0173
WOR	Saint Peter and Saint Paul Parish Church	585444	5819309	Water Orton	$y = 6.28E-05\ X^2 - 3.71E-04\ X + 0$	$R^2 = 0.87$	0.0003	0.0015	0.0028	0.0040	0.0053
WBR	Heath Lane Cemetery	568630	5821123	West Bromwich	$y = 1.26E-04\ X^2 + 1.24E-03\ X + 0$	$R^2 = 0.61$	0.0025	0.0050	0.0075	0.0100	0.0126
WIL	Willenhall Cemetery	565666	5828171	Willenhall	$y = 1.40E-04\ X^2 + 3.64E-04\ X + 0$	$R^2 = 0.59$	0.0018	0.0046	0.0074	0.0102	0.0130
WIT	Witton Cemetery	575877	5820467	Witon	$y = 2.28E-04\ X^2 - 5.44E-04\ X + 0$	$R^2 = 0.83$	0.0007	0.0049	0.0092	0.0134	0.0177

Table2. Name and location of air-quality monitoring stations active within the study area, their location (UTM), and period of record.

Identifier	Site Name (site code)	UTM30 Easting	UTM30 Northing	Start_Date	End_Date	Address
Bil3	BILSTON 3 (330003)	562677	5824589	4/1/1943	4/6/1970	23 WELLINGTON RD, Wolverhampton
Bil18	BILSTON 18 (330018)	562183	5824182	4/4/1978	4/2/1984	ST EDWARDS NURSERY SCHOOL, Wolverhampton
Bil19	BILSTON 19 (330019)	564311	5822211	3/29/1983	3/28/1988	ERNEST BOLD COURT WOLVERHAMPTON ST, Wolverhampton
Bir11	BIRMINGHAM 11 (355011)	577095	5816387	4/3/1962	3/31/1969	CENTRAL LAB, NECHELLS, Birmingham
Bir13	BIRMINGHAM 13 (355013)	576450	5812377	4/3/1962	3/31/1969	CONGREGATIONAL CHURCH, LADYPOOL RD, SPARKBROOK, Birmingham
Bir21	BIRMINGHAM 21 (355021)	575774	5817869	3/28/1972	3/29/1982	ASTON HALL, ASTON PARK, Birmingham
Bir26	BIRMINGHAM 26 (355026)	579387	5817019	4/1/1975	4/3/1995	INGLETON RD JUN & INF SCHOOL, Birmingham
Can15	CANNOCK 15 (530015)	565790	5838135	4/5/1966	4/2/1973	HEALTH DEPT, CHURCH ST, Cannock Chase
Can17	CANNOCK 17 (530017)	564396	5837716	3/28/1972	3/30/1981	LONGFORD COURT, BIDEFORD WAY, Cannock Chase
Can18	CANNOCK 18 (530018)	566470	5839645	4/1/1980	3/30/1998	ARTHUR ST,CHADSMOOR, Cannock Chase
Kid3	KIDDERMINSTER 3 (1680003)	551255	5804326	4/4/1961	4/4/1966	P.H.DEPT, VICAR ST, Wyre Forest
Kid4	KIDDERMINSTER 4 (1680004)	551153	5804525	4/4/1967	4/2/1979	5-9 CHURCH ST, Wyre Forest
Kid5	KIDDERMINSTER 5 (1680005)	551154	5804425	4/3/1979	3/30/1981	26 VICAR ST, Wyre Forest
Old5	OLDBURY 5 (2460005)	566876	5817545	4/1/1958	3/29/1999	MUNICIPAL BUILDINGS, FLASH RD, Sandwell
Row1	ROWLEY REGIS 1 (2752501)	565513	5814826	4/4/1967	3/29/1976	BRITANNIA ROAD SCHOOL, BLACKHEATH, Sandwell
Row2	ROWLEY REGIS 2 (2752502)	565513	5814826	4/1/1975	3/29/1982	CORRIDOR, BRITANNIA RD SCH, BLACKHEATH, Sandwell
Row3	ROWLEY REGIS 3 (2752503)	564299	5815809	3/31/1998	Present	SPRINGFIELD SCHOOL DOULTON ROAD ROWLEY REGIS, Sandwell
Sto1	STOURBRIDGE 1 (3110001)	560246	5812353	4/1/1951	3/29/1982	LYE CLINIC, ORCHARD LANE, Dudley
Wal13	WALSALL 13 (3380013)	567225	5828453	4/4/1961	3/28/1988	BEECHDALE CLINIC, STEPHENSON SQ, LEAMORE, Walsall
Wal18	WALSALL 18 (3380018)	569150	5826679	3/30/1976	Present	ENV. HEALTH DEPT,CIVIC CENTRE,DARWALL ST, Walsall
Wed1	WEDNESFIELD 1 (3470001)	562229	5828084	4/1/1952	3/29/1982	HEALTH CENTRE, HIGH ST, Wolverhampton
Wed2	WEDNESFIELD 2 (3470002)	562329	5828085	3/30/1982	Present	COUNCIL OFFICES,ALFRED SQUIRE RD, Wolverhampton
Wil1	WILLENHALL 1 (3620001)	565047	5826822	4/1/1948	4/6/1970	ALBION WORKS (HARPERS), Walsall
Wil15	WILLENHALL 15 (3620015)	564255	5826211	4/1/1969	3/30/1987	COUNCIL OFFICE, Walsall
Wol3	WOLVERHAMPTON 3 (3660003)	558844	5826936	4/1/1948	3/31/1980	HEALTH OFFICES 57 WATERLOO RD, Wolverhampton
Wol7	WOLVERHAMPTON 7 (3660007)	557590	5823618	4/2/1963	3/30/1987	PENN SCHOOL, MANOR RD, Wolverhampton

Table 3.Results of optimization of parameters, radius, residential land-use indicator, and inverse distance weighting (IDW) power. Maximum values in bold.

Radius

Radius	1960s	1970s	1980s	1990s	2000s
300	0.02	0.01	0.01	0.00	0.02
3000	0.19	0.20	0.19	0.12	0.01
7000	***0.33***	***0.37***	***0.38***	0.28	0.05
8000	0.28	0.33	***0.38***	0.33	0.10
10000	0.22	0.27	0.34	***0.34***	***0.14***

Residential Land-use

Land Use	1960s	1970s	1980s	1990s	2000s
1.0	0.24	0.28	0.34	0.31	0.12
0.8	0.32	0.35	0.41	0.32	0.12
0.6	0.35	0.40	0.43	0.33	0.11
0.4	0.40	0.44	0.45	0.36	0.10
0.2	0.46	0.50	0.49	***0.44***	0.11
0.0	***0.55***	***0.57***	***0.53***	0.35	0.07

IDW Power

IDW	1960s	1970s	1980s	1990s	2000s
2.00	0.00	0.00	0.00	0.01	0.03
1.50	0.00	0.00	0.00	0.01	0.03
1.00	0.00	0.00	0.00	0.01	0.03
0.50	0.02	0.02	0.01	0.00	0.01
0.40	0.17	0.18	0.16	0.09	0.00
0.25	***0.33***	0.36	0.37	0.26	0.04
0.00	***0.33***	***0.37***	***0.39***	***0.29***	0.06

Table 4. Correlation coefficients for land-use using the point-density calculation vs. average decadal gravestone stone decay rate for radii of 4000 – 12000 m. Maximum values in bold/italic

Resid. Ind.	Radius	1960s	1970s	1980s	1990s	2000s
Residential Value 0.2						
0.2	4000	0.45	0.48	0.47	0.32	0.06
0.2	6000	***0.56***	***0.60***	***0.59***	0.40	0.07
0.2	7000	0.53	0.58	***0.59***	0.43	0.10
0.2	8000	0.45	0.51	0.55	0.44	0.12
0.2	10000	0.37	0.44	0.49	0.43	***0.14***
0.2	12000	0.34	0.42	0.48	0.42	0.14
Residential Value 0.0						
0.0	4000	0.45	0.45	0.40	0.23	0.02
0.0	6000	***0.65***	0.66	0.60	0.34	0.03
0.0	7000	**0.65**	***0.68***	***0.65***	0.41	0.06
0.0	8000	0.52	0.58	0.60	***0.45***	0.10
0.0	10000	0.38	0.44	0.48	0.41	***0.14***
0.0	12000	0.33	0.40	0.46	0.40	0.14

Table 5. Correlation coefficients for gravestone decay and land use for each directional search window. Maximum values in bold/italic with near maximum values in grey.

Azimuth	1960s	1970s	1980s	1990s	2000s
0	0.01	0.02	0.05	0.12	0.14
45	0.00	0.00	0.00	0.01	0.05
90	0.13	0.14	0.14	0.12	0.04
135	***0.39***	0.38	0.33	0.16	0.00
180	0.33	0.26	0.14	0.01	0.06
225	0.31	0.27	0.18	0.03	0.03
270	0.32	***0.39***	***0.44***	0.34	0.06
315	0.15	0.23	0.33	***0.39***	0.19
0	0.10	0.16	0.26	0.33	***0.20***
45	0.00	0.00	0.01	0.04	0.09
135	***0.45***	0.41	0.29	0.09	0.01
135	0.15	0.15	0.14	0.11	0.03
225	0.31	0.27	0.18	0.03	0.03
270	0.36	***0.44***	***0.51***	***0.41***	0.09
0	0.08	0.12	0.19	0.27	***0.20***
45	0.12	0.13	0.15	0.15	0.08
135	0.35	0.31	0.23	0.09	0.00
180	***0.52***	***0.49***	0.37	0.13	0.01
225	0.46	***0.49***	0.45	0.24	0.01
315	0.29	0.37	***0.46***	***0.43***	0.14

Table 6. Mean decadal SO_2 and smoke concentrations ($\mu g/m^3$) for 23 air-quality monitoring stations in the study area. Interpolated land-use indicator determined by point-density function.

site_name	Land Use Indicator	1960s SO2	1960s Smoke	1970s SO2	1970s Smoke	1980s SO2	1980s Smoke
BILSTON 3	0.56	99.00	128.00	-	-	-	-
BILSTON 18	0.55	-	-	64.50	29.00	40.67	25.00
BILSTON 19	0.64	-	-	-	-	42.60	15.60
BIRMINGHAM 11	0.55	277.33	131.17	-	-	-	-
BIRMINGHAM 13	0.46	202.40	125.20	-	-	-	-
BIRMINGHAM 21	0.55	-	-	101.86	27.57	75.00	22.67
BIRMINGHAM 26	0.52	-	-	100.00	28.60	46.50	15.30
CANNOCK 15	0.07	103.50	103.50	-	-	-	-
CANNOCK 17	0.07	-	-	88.33	65.50	54.13	50.88
CANNOCK 18	0.06	-	-	-	-	-	-
KIDDERMINSTER 3	0.07	167.33	112.75	-	-	-	-
KIDDERMINSTER 4	0.06	60.00	60.00	47.14	14.86	-	-
KIDDERMINSTER 5	0.07	-	-	72.00	13.00	-	-
OLDBURY 5	0.50	127.71	94.29	108.70	37.90	116.00	25.67
ROWLEY REGIS 1	0.46	126.33	64.00	86.80	44.40	-	-
ROWLEY REGIS 2	0.46	-	-	58.80	22.00	63.33	14.67
ROWLEY REGIS 3	0.50	-	-	-	-	-	-
STOURBRIDGE 1	0.24	115.33	84.00	82.13	34.44	66.00	24.33
WALSALL 13	0.33	155.50	111.63	78.60	50.00	44.22	26.78
WALSALL 18	0.32	-	-	81.33	29.33	46.44	21.56
WEDNESFIELD 1	0.43	117.50	117.50	79.00	46.20	81.00	30.00
WEDNESFIELD 2	0.43	-	-	-	-	44.75	15.38
WILLENHALL 1	0.52	159.67	132.75	-	-	-	-
WILLENHALL 15	0.53	-	-	113.40	42.70	52.50	26.00
WOLVERHAMPTON 3	0.33	118.71	109.43	85.50	43.90	-	-
WOLVERHAMPTON 7	0.33	102.67	85.00	54.83	23.33	52.63	13.38